

1 **Virological characteristics of the SARS-CoV-2 KP.2 variant**

2
3 Yu Kaku^{1#}, Keiya Uriu^{1#}, Yusuke Kosugi^{1,2#}, Kaho Okumura^{1,3#}, Daichi
4 Yamasoba^{1,4}, Yoshifumi Uwamino⁵, Jin Kuramochi^{6,7}, Kenji Sadamasu⁸,
5 Kazuhisa Yoshimura⁸, Hiroyuki Asakura⁸, Mami Nagashima⁸, The Genotype to
6 Phenotype Japan (G2P-Japan) Consortium, Jumpei Ito^{1,9}, Kei Sato^{1,2,9,10,11,12,13*}

7
8 ¹ Division of Systems Virology, Department of Microbiology and Immunology, The
9 Institute of Medical Science, The University of Tokyo, Tokyo, Japan

10 ² Graduate School of Medicine, The University of Tokyo, Tokyo, Japan

11 ³ Faculty of Liberal Arts, Sophia University, Tokyo, Japan

12 ⁴ Faculty of Medicine, Kobe University, Kobe, Japan

13 ⁵ Department of Laboratory Medicine, Keio University School of Medicine, Tokyo,
14 Japan

15 ⁶ Interpark Kuramochi Clinic, Utsunomiya, Japan

16 ⁷ Department of Global Health Promotion, Tokyo Medical and Dental University,
17 Tokyo, Japan

18 ⁸ Tokyo Metropolitan Institute of Public Health, Tokyo, Japan

19 ⁹ International Research Center for Infectious Diseases, The Institute of Medical
20 Science, The University of Tokyo, Tokyo, Japan

21 ¹⁰ International Vaccine Design Center, The Institute of Medical Science, The
22 University of Tokyo, Tokyo, Japan

23 ¹¹ Graduate School of Frontier Sciences, The University of Tokyo, Kashiwa, Japan

24 ¹² Collaboration Unit for Infection, Joint Research Center for Human Retrovirus
25 infection, Kumamoto University, Kumamoto, Japan

26 ¹³ MRC-University of Glasgow Centre for Virus Research, Glasgow, UK

27
28 # Contributed equally to this study.

29 *Correspondence: KeiSato@g.ecc.u-tokyo.ac.jp (Kei Sato)

30
31 Word count: 318/500 words, 2/8 references

33 **Abstract**

34 The JN.1 variant (BA.2.86.1.1), arising from BA.2.86(.1) with the S:L455S
35 substitution, exhibited increased fitness and outcompeted the previous dominant
36 XBB lineage by the biggening of 2024. JN.1 subsequently diversified, leading to
37 the emergence of descendants with spike (S) protein substitutions such as
38 S:R346T and S:F456L. Particularly, the KP.2 (JN.1.11.1.2) variant, a descendant
39 of JN.1 bearing both S:R346T and S:F456L, is rapidly spreading in multiple
40 regions as of April 2024. Here, we investigated the virological properties of KP.2.
41 KP.2 has three substitutions in the S protein including the two above and
42 additional one substitution in non-S protein compared with JN.1. We estimated
43 the relative effective reproduction number (R_e) of KP.2 based on the genome
44 surveillance data from the USA, United Kingdom, and Canada where >30
45 sequences of KP.2 has been reported, using a Bayesian multinomial logistic
46 model. The R_e of KP.2 is 1.22-, 1.32-, and 1.26-times higher than that of JN.1 in
47 USA, United Kingdom, and Canada, respectively. These results suggest that KP.2
48 has higher viral fitness and potentially becomes the predominant lineage
49 worldwide. Indeed, as of the beginning of April 2024, the estimated variant
50 frequency of KP.2 has already reached 20% in United Kingdom.

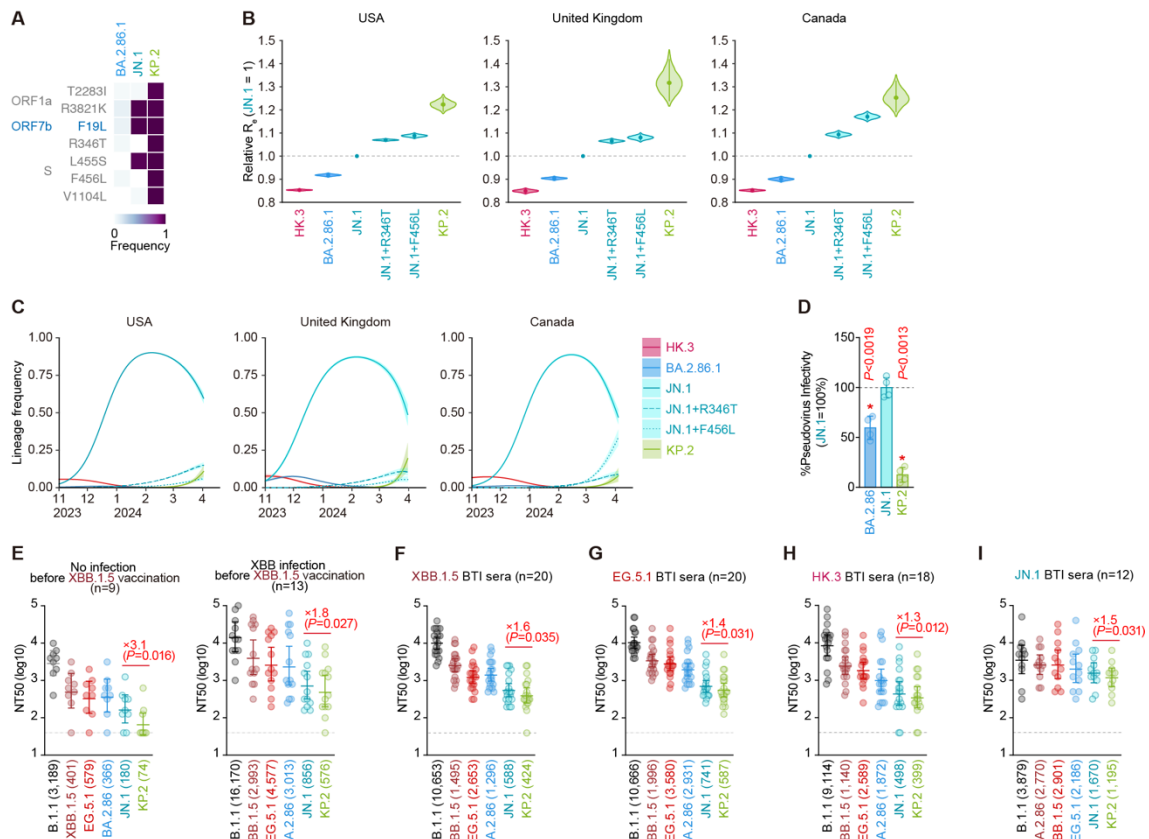
51 The pseudovirus assay showed that the infectivity of KP.2 is significantly
52 (10.5-fold) lower than that of JN.1. We then performed a neutralization assay
53 using monovalent XBB.1.5 vaccine sera and breakthrough infection (BTI) sera
54 with XBB.1.5, EG.5, HK.3 and JN.1 infections. In all cases, the 50% neutralization
55 titer (NT_{50}) against KP.2 was significantly lower than that against JN.1. Particularly,
56 KP.2 shows the most significant resistance to the sera of monovalent XBB.1.5
57 vaccinee without infection (3.1-fold) as well as those who with infection (1.8-fold).
58 Altogether, these results suggest that the increased immune resistance ability of
59 KP.2 partially contributes to the higher R_e more than previous variants including
60 JN.1.

61 **Text**

62 The JN.1 variant (BA.2.86.1.1), arising from BA.2.86(1) with the S:L455S
63 substitution, exhibited increased fitness and outcompeted the previous dominant
64 XBB lineage by the biggining of 2024.¹ JN.1 subsequently diversified, leading to
65 the emergence of descendants with spike (S) protein substitutions such as
66 S:R346T and S:F456L. Particularly, the KP.2 (JN.1.11.1.2) variant, a descendant
67 of JN.1 bearing both S:R346T and S:F456L, is rapidly spreading in multiple
68 regions as of April 2024. Here, we investigated the virological properties of KP.2.
69 KP.2 has three substitutions in the S protein including the two above and
70 additional one substitution in non-S protein compared with JN.1 (**Figure 1A**). We
71 estimated the relative effective reproduction number (R_e) of KP.2 based on the
72 genome surveillance data from the USA, United Kingdom, and Canada where
73 >30 sequences of KP.2 has been reported, using a Bayesian multinomial logistic
74 model (**Figures 1B and 1C; Table S3**).² The R_e of KP.2 is 1.22-, 1.32-, and 1.26-
75 times higher than that of JN.1 in USA, United Kingdom, and Canada, respectively
76 (**Figure 1B**). These results suggest that KP.2 has higher viral fitness and
77 potentially becomes the predominant lineage worldwide. Indeed, as of the
78 beginning of April 2024, the estimated variant frequency of KP.2 has already
79 reached 20% in United Kingdom (**Figure 1C**).

80 The pseudovirus assay showed that the infectivity of KP.2 is significantly
81 (10.5-fold) lower than that of JN.1 (**Figure 1D**). We then performed a
82 neutralization assay using monovalent XBB.1.5 vaccine sera and breakthrough
83 infection (BTI) sera with XBB.1.5, EG.5, HK.3 and JN.1 infections. In all cases,
84 the 50% neutralization titer (NT_{50}) against KP.2 was significantly lower than that
85 against JN.1 (**Figures 1E-I**). Particularly, KP.2 shows the most significant
86 resistance to the sera of monovalent XBB.1.5 vaccinee without infection (3.1-fold)
87 as well as those who with infection (1.8-fold) (**Figures 1E**). Altogether, these
88 results suggest that the increased immune resistance ability of KP.2 partially
89 contributes to the higher R_e more than previous variants including JN.1.

90



91
 92 **Figure 1. Virological features of KP.2**
 93 (A) Frequency of mutations in KP.2 and other lineages of interest. Only mutations
 94 with a frequency >0.5 in at least one but not all the representative lineages are
 95 shown.
 96 (B) Estimated relative R_e of the variants of interest in the USA, United Kingdom,
 97 and Canada. The relative R_e of JN.1 is set to 1 (horizontal dashed line). Violin,
 98 posterior distribution; dot, posterior mean; line, 95% Bayesian confidence interval.
 99 (C) Estimated epidemic dynamics of the variants of interest in the USA, United
 100 Kingdom, and Canada from November 1, 2023 to April 11, 2024. Countries are
 101 ordered according to the number of detected sequences of KP.2 from high to low.
 102 Line, posterior mean, ribbon, 95% Bayesian confidence interval.
 103 (D) Lentivirus-based pseudovirus assay. HOS-ACE2/TMPRSS2 cells were
 104 infected with pseudoviruses bearing each S protein of BA.2.86, JN.1 and KP.2.
 105 The amount of input virus was normalized to the amount of HIV-1 p24 capsid
 106 protein. The percentage infectivity of BA.2.86 and KP.2 are compared to that of
 107 JN.1. The horizontal dash line indicates the mean value of the percentage
 108 infectivity of JN.1. Assays were performed in quadruplicate, and a representative
 109 result of four independent assays is shown. The presented data are expressed
 110 as the average \pm SD. Each dot indicates the result of an individual replicate.
 111 Statistically significant differences versus JN.1 is determined by two-sided
 112 Student's t tests (*, $P < 0.01$).
 113 (E-I) Neutralization assay. Assays were performed with pseudoviruses harboring
 114 the S proteins of B.1.1, XBB.1.5, EG.5.1, BA.2.86, JN.1 and KP.2. The following
 115 sera were used: vaccinated sera from fully vaccinated individuals who had not

116 been infected (9 donors) and vaccinated sera from fully vaccinated individuals
117 who had been infected with XBB subvariants (after June, 2023) (13 donors) (**E**);
118 convalescent sera from fully vaccinated individuals who had been infected with
119 XBB.1.5 (one 2-dose vaccinated donor, seven 3-dose vaccinated donors, six 4-
120 dose vaccinated donors, five 5-dose vaccinated donors and one 6-dose
121 vaccinated donor. 20 donors in total) (**F**); EG.5.1 (one 2-dose vaccinated donor,
122 six 3-dose vaccinated donors, five 4-dose vaccinated donors, four 5-dose
123 vaccinated donors and four 6-dose vaccinated donors. 20 donors in total) (**G**);
124 individuals who had been infected with HK.3 (three 2-dose vaccinated donors,
125 five 3-dose vaccinated donor, two 4-dose vaccinated donors, three 5-dose
126 vaccinated donors, one 6-dose vaccinated donor and four donors with unknown
127 vaccine history. 18 donors in total) (**H**) and individuals who had been infected with
128 JN.1 (one 2-dose vaccinated donor, two 3-dose vaccinated donors, two 7-dose
129 vaccinated donors and seven donors with unknown vaccine history. 12 donors in
130 total) (**I**). Assays for each serum sample were performed in quadruplicate to
131 determine the 50% neutralization titer (NT₅₀). Each dot represents one NT₅₀ value,
132 and the geometric mean and 95% confidence interval are shown. The number in
133 parenthesis indicates the geometric mean of NT₅₀ values. The horizontal dash
134 line indicates the detection limit (40-fold). Statistically significant differences
135 versus KP.2 were determined by two-sided Wilcoxon signed-rank tests, and p
136 values are indicated in parentheses. The fold changes of NT₅₀ from that of KP.2
137 are indicated with “X”.

138

139 **Grants**

140 Supported in part by AMED ASPIRE Program (JP24jf0126002, to G2P-Japan
141 Consortium and Kei Sato); AMED SCARDA Japan Initiative for World-leading
142 Vaccine Research and Development Centers "UTOPIA" (JP243fa627001h0003,
143 to Kei Sato); AMED SCARDA Program on R&D of new generation vaccine
144 including new modality application (JP243fa727002h0003, to Kei Sato); AMED
145 Research Program on Emerging and Re-emerging Infectious Diseases
146 (JP243fa727002, to Kei Sato); JST PRESTO (JPMJPR22R1, to Jumpei Ito);
147 JSPS KAKENHI Grant-in-Aid for Early-Career Scientists (JP23K14526, to
148 Jumpei Ito); JSPS KAKENHI Grant-in-Aid for Scientific Research A (JP24H00607,
149 to Kei Sato); JSPS Research Fellow DC2 (JP22J11578, to Keiya Uriu); JSPS
150 Research Fellow DC1 (JP23KJ0710, to Yusuke Kosugi); The Tokyo Biochemical
151 Research Foundation (to Kei Sato); The Mitsubishi Foundation (to Kei Sato).

152

153 **Declaration of interest**

154 J.I. has consulting fees and honoraria for lectures from Takeda Pharmaceutical
155 Co. Ltd. K.S. has consulting fees from Moderna Japan Co., Ltd. and Takeda
156 Pharmaceutical Co. Ltd. and honoraria for lectures from Gilead Sciences, Inc.,
157 Moderna Japan Co., Ltd., and Shionogi & Co., Ltd. The other authors declare no
158 competing interests. All authors have submitted the ICMJE Form for Disclosure
159 of Potential Conflicts of Interest. Conflicts that the editors consider relevant to the
160 content of the manuscript have been disclosed.

161 **References**

162 1. Kaku Y, Okumura K, Padilla-Blanco M, *et al.* Virological characteristics of the
163 SARS-CoV-2 JN.1 variant. *Lancet Infect Dis* 2024; published online Jan 3.
164 DOI:10.1016/S1473-3099(23)00813-7.

165 2. Yamasoba D, Kimura I, Nasser H, *et al.* Virological characteristics of the
166 SARS-CoV-2 Omicron BA.2 spike. *Cell* 2022; **185**: 2103-2115.e19.

167